Supplementary information

This document contains an x-ray diffractogram of $Li_2B_{12}H_{12}$, the time evolution of the Boron and Lithium K-edge XRS of the $LiBH_4$/C as prepared, B and Li K-edge XRS of reference materials, details on the deconvolution analyses of the boron and Lithium K-edge XRS of $LiBH_4$/C deh and $LiBH_4$/C reh, and C K-edge XRS of $LiBH_4$/C under different conditions. The oxygen K-edge XRS of two samples is shown as well.

In addition it shows the B and C K-edge XRS data measured for nanoconfined $NaBH_4$ ($NaBH_4$/C) and XAS calculations of the $NaBH_4$ and $Na_2B_{12}H_{12}$ and C K-edge XRS of both $NaBH_4$/C and $LiBH_4$/C under different conditions.

1. XRD of $Li_2B_{12}H_{12}$

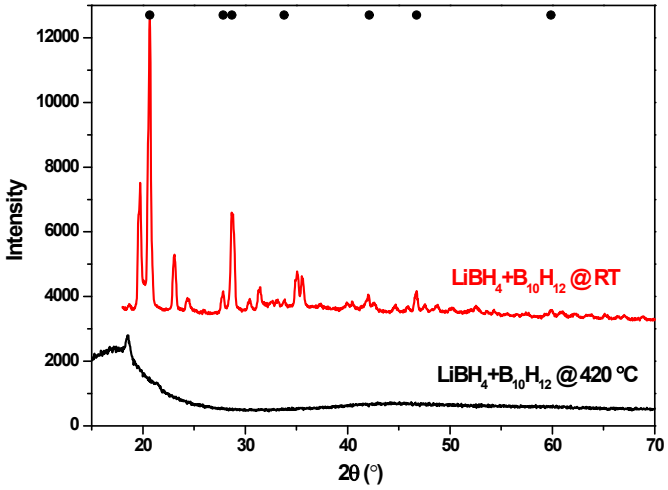

Figure S1. XRD patterns of a mixture of $LiBH_4$ and $B_{10}H_{12}$ at room temperature (red) and after reaction at 420 °C (black). The XRD characteristics for LiBH4 are indicated with black bullets.

2. Time evolution of the B and Li K-edge XRS of the LiBH4/C as prep.

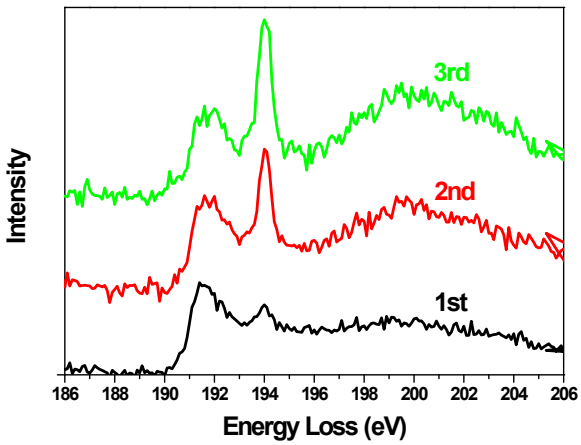

Figure S2. Time-evolving B K-edge of $LiBH_4$/C as prepared with intervals of approximately half an hour.

Note the increasing peak at 194 eV in the B K-edge XRS in Figure S2, indicating an increase in oxidic boron, while the Li K-edge XRS does not change accordingly as seen in Figure S3 in the same time period.

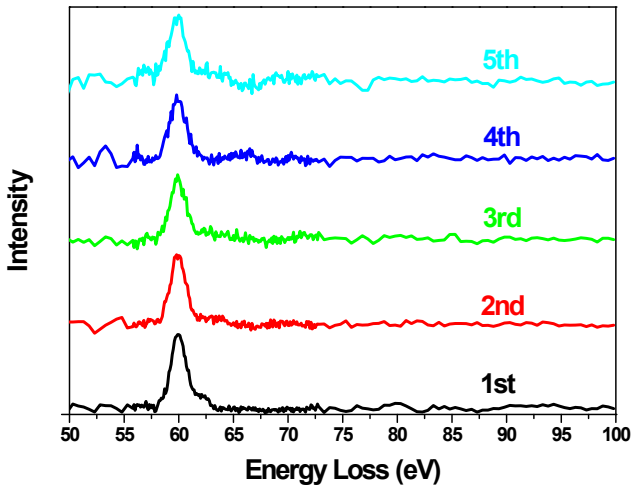

Figure S3. Time-evolving Li K-edge XRS of $LiBH_4$/C as prepared with intervals of approximately half an hour.

3. Boron K-edge XRS of reference materials

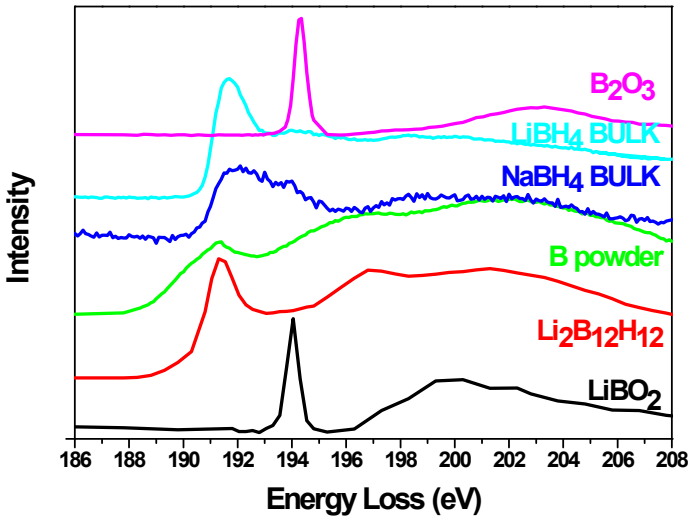

Figure S4. Boron K-edge XRS of the reference compounds $LiBO_2$ (black), $Li_2B_{12}H_{12}$ (red), boron powder (B powder, green), bulk $NaBH_4$ powder (blue), bulk $LiBH_4$ powder (cyan) and B_2O_3 (magenta).

The B K-edge XRS of $LiBO_2$, $Li_2B_{12}H_{12}$, boron, bulk $NaBH_4$, bulk $LiBH_4$ and B_2O_3 are shown in figure S4. The first structure occurs in the range of 188 eV to196 eV and depends on the electronic structure around the boron: it corresponds to the excitation of the boron 1s electron to the lowest unoccupied (2p) states. The energy at which this happens is different for the different reference materials because the electronic structure of B in these compounds depends largely on the charges or electro-negativity of the bonding element(s). For example the B K-edge XRS of B_2O_3 and $LiBO_2$ are similar, which indicates that the sharp peak at ~194 eV accounts for oxidic boron, i.e. to rather positive ionic B^{3+} cations. The band at higher energy (above 197 eV) is different for these two different oxidic boron compounds which may provide useful means of differentiating between the different

oxidic species of boron in XRS. Generally the peak at lowest energy loss follows the boron oxidation state or more precisely the electronic charge on the B. The first peak appears at lowest energy loss for boron powder (and $Li_2B_{12}H_{12}$) and highest energy loss in the compounds with higher overall charge on the boron such as in the oxides. Although B has a formal +3 oxidation state in $NaBH_4$, $LiBH_4$, $LiBO_2$ and B_2O_3, the boron atoms in the oxides are more positively charged than for the borohydrides due to the high electro-negativity of oxygen. As well, the hydrogen atoms bind more covalently to the boron, thus the boron is only formally in the +3 oxidation state in the borohydrides. The boron atom in $LiBH_4$ is slightly more negatively charged than for $NaBH_4$ due to slightly higher electro-negativity of Li compared to Na. Therefore the peak is observed at slightly lower energy for $LiBH_4$ than for $NaBH_4$.

4. Analysis of the Boron K-edge XRS from deconvolution in reference spectra

In order to compare the experiments of the LiBH4/C under different conditions with reference spectra, the reference spectra have to be normalized in some way. Since the amount of powder that was pressed in the sample holder was not always the same, we have made use of the following assumptions:

(1) The area of the XRS spectrum between two fixed energies (with same intensity) corresponds to the total of locally boron unoccupied states of the material and therefore the XRS areas in figure S5 correspond to the same boron content in the different materials.
(2) The obtained area of the unoccupied states has to be divided by the amount of boron atoms present (12 in the case of $Li_2B_{12}H_{12}$) to provide the relative amount of material present; in our deconvolution analyses we present the weight % so also the total molecular weight of the material is taken into account.

The B K-edge spectra of the references $LiBH_4$, $Li_2B_{12}H_{12}$ and boron powder were set to zero at 185 eV and the step at 237 eV was set to 0.32 for the three compounds, leading to the result in Figure S5. As said, these spectra relate to each other as having the same atomic boron content.

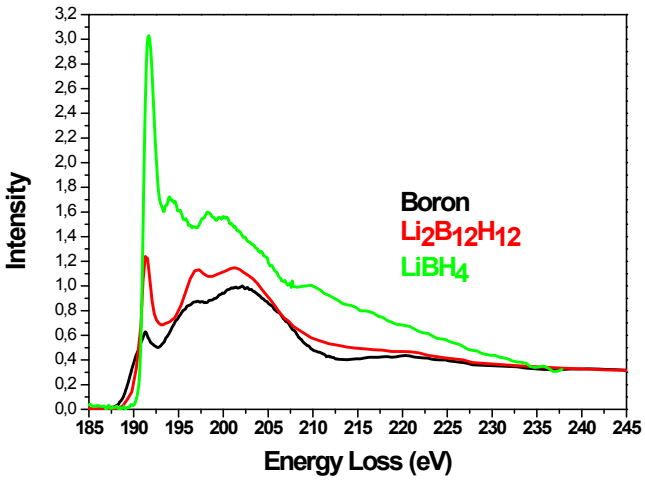

Figure S5. Boron K-edge XRS of boron (black), $Li_2B_{12}H_{12}$ (red) and $LiBH_4$ (green) with the pre-edge plateau at 185 eV set to zero intensity and the step at 237 eV was set to an intensity of 0.32.

Note that we do not speak here about normalization of the B K-edge XRS spectra of the nanoconfined materials. The relative weight of the references is only normalized in this way to get an estimate of the relative weight% of the different materials in the deconvolution analysis. In particular the XRS spectra of LiBH4/C are commonly normalized on the maximum intensity.

The B K-edge XRS spectra shown in Figure S6, Figure S7 and Figure S8 are comparisons between combinations of different reference compounds with the nanoconfined $LiBH_4$ at different stages of the de- and re-hydrogenation: $LiBH_4$/C deh., $LiBH_4$/C+part. reh.H_2 and $LiBH_4$/C reh.

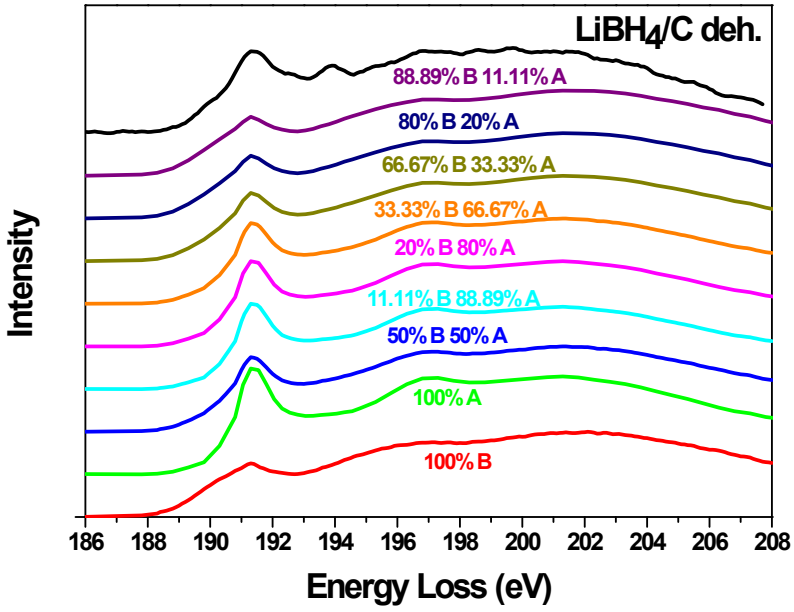

Figure S6. Boron K-edge XRS spectra of $LiBH_4$/C de-hydrogenated ($LiBH_4$/C deh., black) and mixtures of the references A=$Li_2B_{12}H_{12}$ and B=boron powder after their pre-edge plateaus and edge jump were normalized to each other as done in the Supporting Information, Figure S5.

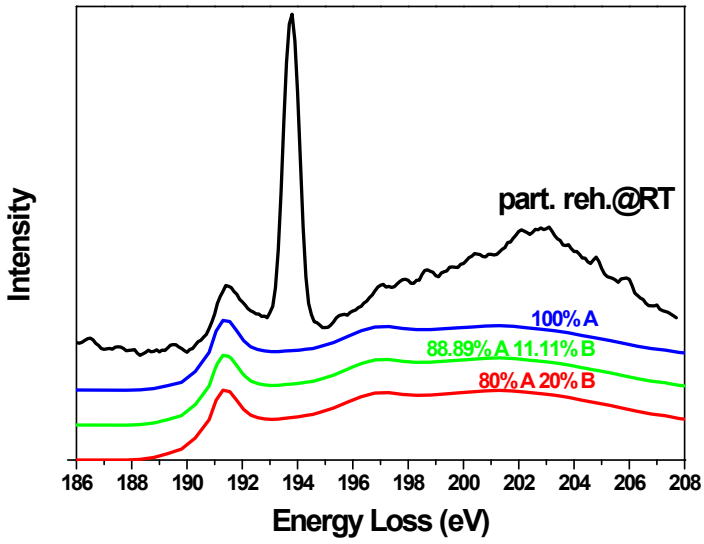

Figure S7. Boron K-edge XRS of $LiBH_4$/C de-hydrogenated and subsequently partially re-hydrogenated in-situ under 1 bar of hydrogen measured at room temperature (part. reh.@RT, black) and XRS of combinations of A=$Li_2B_{12}H_{12}$ and B=boron powder and XRS of 100% A. Note that the agreement of the shown combinations with the experimental data is not good enough at the main peak, that is without adding $LiBH_4$ to the combination.

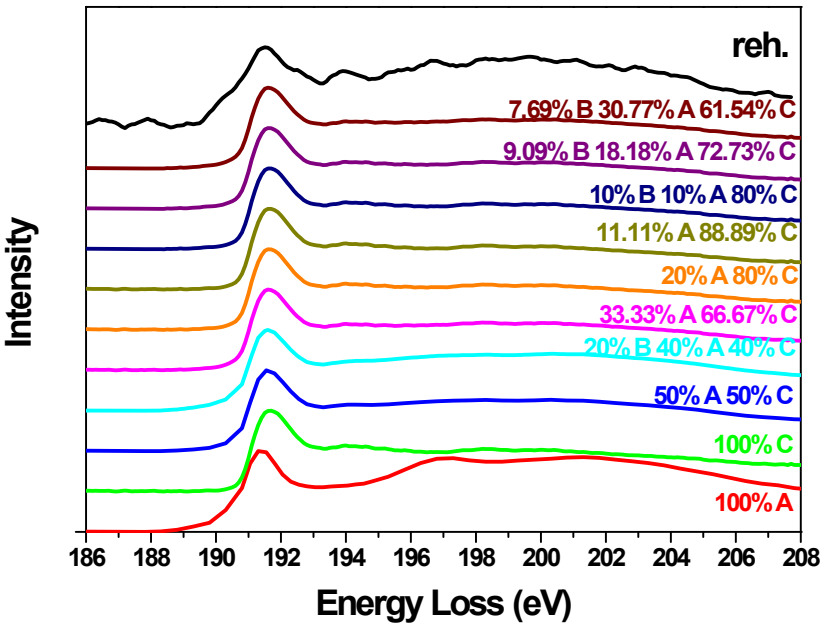

Figure S8. Boron K-edge XRS of re-hydrogenated $LiBH_4$/C (reh., black) compared to some mixtures in atom percentages of A=$Li_2B_{12}H_{12}$, B= boron powder and C=$LiBH_4$ bulk powder references as from Figure S5.

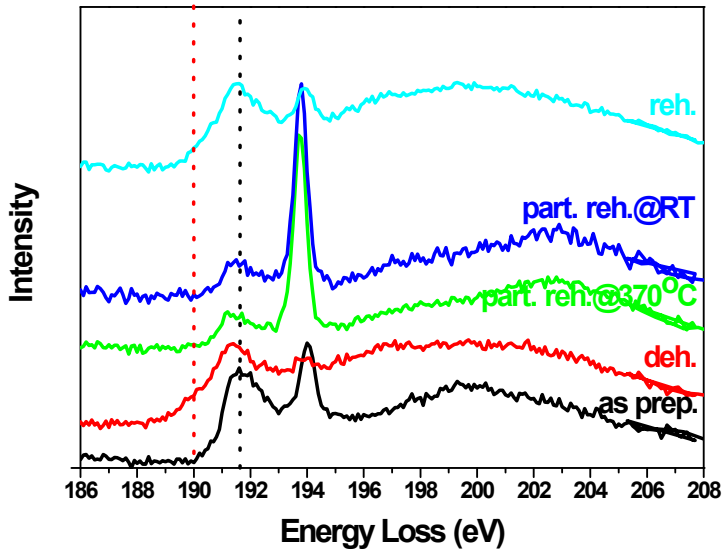

Figure S9. Boron K-edge XRS of $LiBH_4$/C as prepared (as prep., black), de-hydrogenated $LiBH_4$/C (deh., red), partially re-hydrogenated $LiBH_4$/C at 370°C (part. reh@370oC, green) and at room temperature after cooling down (part. reh@RT, blue) and the $LiBH_4$/C de-hydrogenated and subsequently re-hydrogenated ex-situ (reh. light blue).

5. Li K-edges of $LiBH_4$/C under different conditions and Li K-edges of references

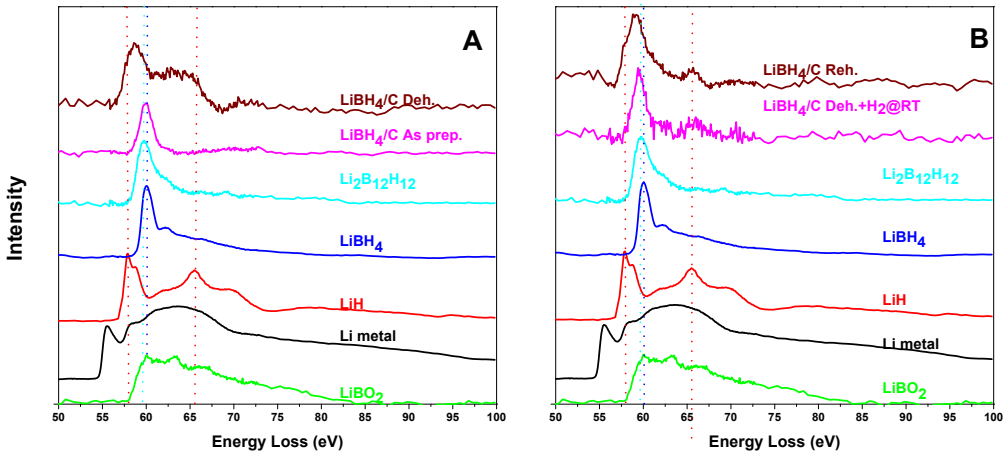

Figure S10. Lithium K-edge XRS of the reference materials lithium metal (Li metal, black line) lithium hydride powder (LiH, red line), bulk lithium borohydride powder ($LiBH_4$, blue), lithium metaborate powder ($LiBO_2$, green) and $Li_2B_{12}H_{12}$ (light blue) in both panels A and B compared with lithium K-edge XRS of the samples $LiBH_4$/C as prepared ($LiBH_4$/C as prep., pink panel A), and $LiBH_4$ de-hydrogenated ex-situ (deh., brown panel A) in panel A, and de-hydrogenated and subsequently partially re-hydrogenated in-situ by heating under 1 bar of hydrogen to 370°C and after a dwell time of 30 minutes cooled down to room temperature (part. reh.@RT, pink panel B) and $LiBH_4$/C re-hydrogenated ex-situ (reh., brown panel B) shown in panel B.

6. Analysis Li K-edge from deconvolution in reference spectra

As for the B K-edge, the Li K-edge XRS spectra of the reference materials have to be normalized to each other. For the analysis of the Li K-edge the references were adjusted such that the onset at an energy loss of 55 eV was zero and the step was set to one particular value. These are then the reference spectra that can be related to each other having the same amount of Lithium atoms. Note the relative intensities of $Li_2B_{12}H_{12}$ and LiH with $LiBH_4$ in Figure S11.

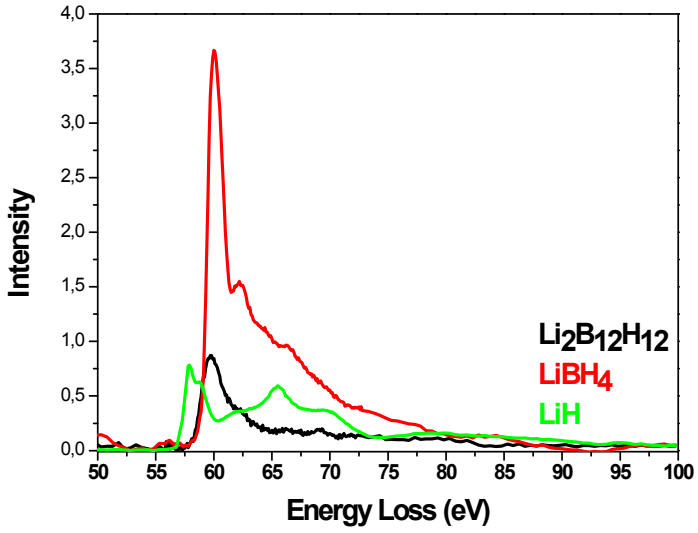

Figure S11. Li K-edge XRS of $Li_2B_{12}H_{12}$ (black), $LiBH_4$ (red) and LiH (green) with the pre-edge plateau at 55 eV set to zero intensity and the step (at 98 eV) was set to an intensity of 0.04.

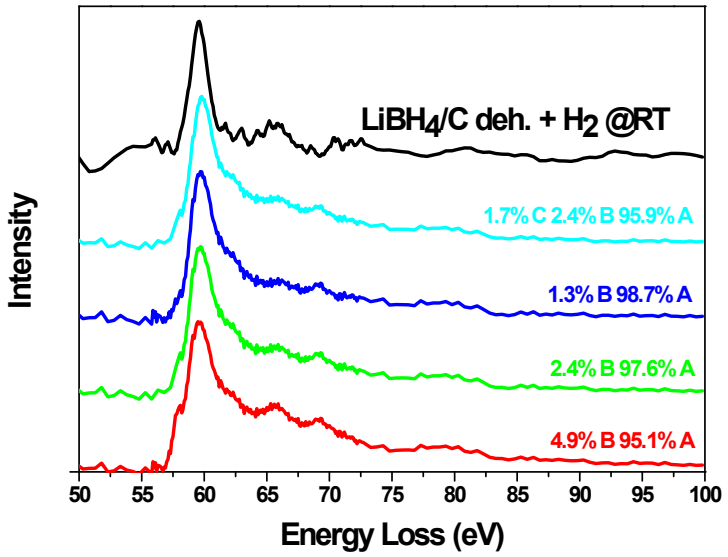

Figure S12. Li K-edge XRS of $LiBH_4$/C de-hydrogenated ex-situ and subsequently partially re-hydrogenated in-situ under 1 bar of hydrogen ($LiBH_4$/C deh.+H_2@RT, black) and XRS with some combinations of the references A=$Li_2B_{12}H_{12}$, B=LiH and C=$LiBH_4$ (with the original references normalized to each other as reported in the Supporting Information, Figure S11 and the percentages presented in the figure are related to different amounts of the references).

Comparing different percentages of the Li K-edge XRS of the bulk $LiBH_4$ (C), LiH (B) and $Li_2B_{12}H_{12}$ (A) references with the experimental Li K-edge XRS of $LiBH_4$/C deh.+H_2@RT (black line in Figure S12) it is concluded that the $LiBH_4$/C deh.+H_2@RT is a combination of the relative amounts of the different references: about 95±3 % $Li_2B_{12}H_{12}$ and 5±3% of LiH and approximately 2% of $LiBH_4$.

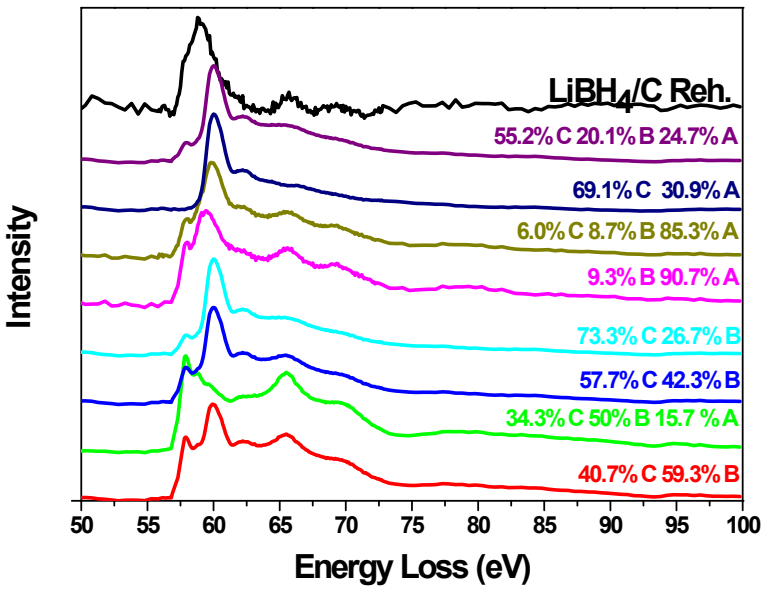

Figure S13. Li K-edge XRS of $LiBH_4$/C re-hydrogenated ex-situ ($LiBH_4$/C reh., black) with a combination of references A=$Li_2B_{12}H_{12}$, B=LiH, C=$LiBH_4$ bulk powders (with the original references normalized to each other as reported in supporting information, Figure S11 and the percentages related to the different amounts of the references).

According to Figure S13 there can be up to 20.0±20% LiH and also 20±20% $Li_2B_{12}H_{12}$ and 60.0±20% $LiBH_4$ present in the Li K-edge XRS of $LiBH_4$/C reh. Note that the errors are larger than the previous deconvolution and that is because the correspondence between the experimental Li K-edge XRS of $LiBH_4$/C reh and the combinations of $LiBH_4$, $Li_2B_{12}H_{12}$ and LiH is lower than for the XRS of combinations of these references with the XRS of $LiBH_4$/C deh.+H_2@RT.

Summarizing, the Li K-edge XRS of $LiBH_4$/C as prep agrees with the Li K-edge XRS of the bulk $LiBH_4$ powder. From the deconvolution processes on the Li K-edge XRS, it is found that the $LiBH_4$/C part. reh.@RT contains about 95±3 % $Li_2B_{12}H_{12}$ and 5±3% of LiH and maybe a little (~2%) of $LiBH_4$, while according to an analysis of the Li K-edge XRS of $LiBH_4$/C reh., the re-hydrogenated sample contains 20±20% of both LiH and $Li_2B_{12}H_{12}$ and 60±20% $LiBH_4$. This shows that the first re-hydrogenation step leads to $Li_2B_{12}H_{12}$, while the full re-hydrogenation, with higher hydrogen pressures and higher temperatures, leads to $LiBH_4$ and interestingly some LiH and also possibly still some small portion of $Li_2B_{12}H_{12}$. The LiH in the full re-hydrogenation may partially be related to the lithium that is intercalated in the carbon structure after dehydrogenation and does not yet become LiH or $Li_2B_{12}H_{12}$ in the partial re-hydrogenation step with 1 bar of hydrogen, but with higher hydrogen pressures these intercalated lithium might set free and bind to hydrogen forming LiH.

7. B K-edge deconvolution of $LiBH_4$/C at different stages of de- and re-hydrogenation

Figure S14 shows some of the best fits of deconvolution of de-hydrogenated $LiBH_4$/C ($LiBH_4$/C deh. black, panel A), de-hydrogenated $LiBH_4$/C after hydrogenation with 1 bar of hydrogen ($LiBH_4$/C deh.+H_2@RT black, panel B) and ex-situ re-hydrogenated $LiBH_4$/C ($LiBH_4$/C Reh., black, panel C). Since these deconvolution fits do not necessarily differ from each other in their fitting to the experimental data, we could identify the error bars mentioned in the main paper.

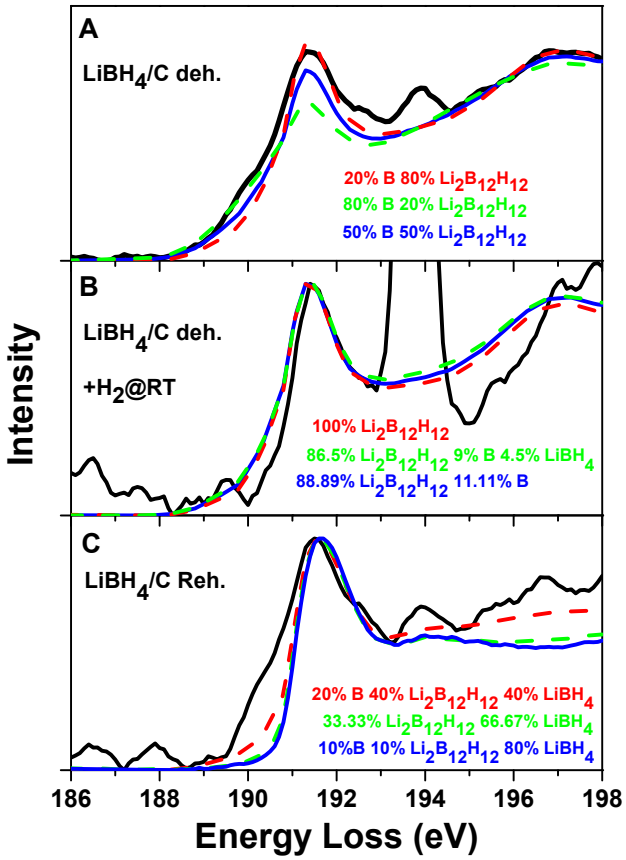

Figure S14. Best fits from the deconvolution of the B K-edge XRS of (A) $LiBH_4$/C deh, (B) $LiBH_4$/C deh+H_2@RT and (C) $LiBH_4$/C Reh. Black lines correspond to the experimental B K-edge XRS of the $LiBH_4$/C at different points in the re-hydrogenation and blue lines are the best convolution fit with their different percentages of reference materials. The red and green dotted lines are other representative combinations of reference spectra marking the error bars.

8. O K-edge of $LiBH_4$/C Deh. and Deh.+H_2@RT

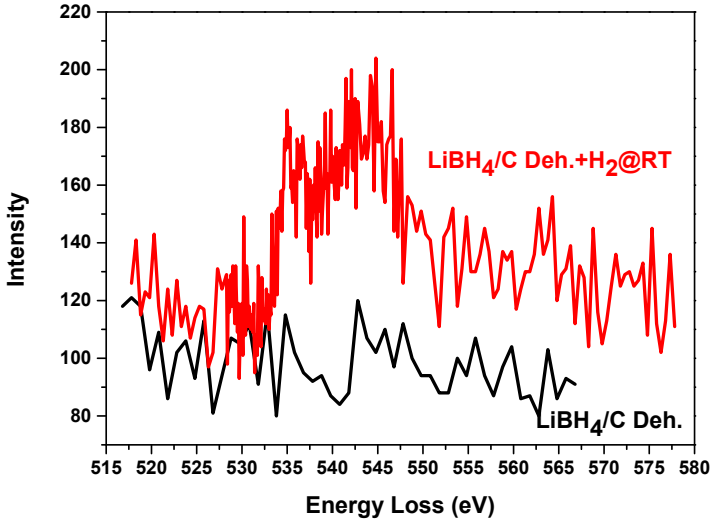

Figure S15. Oxygen K-edge XRS of $LiBH_4$/C Deh. (black) and $LiBH_4$/C deh.+H_2@RT (red).

As the B K-edge XRS spectra showed increased features assigned to oxygenated boron species, we also measured oxygen K-edge XRS for some samples. In Figure S15 the oxygen K-edge spectra for $LiBH_4$/C deh. (black) and $LiBH_4$/C ex-situ dehydrogenated and subsequently in-situ heated under H_2 flow and cooled down after ($LiBH_4$/C Deh.+H_2@RT, red) are shown. Although these spectra are noisy, they indicate the same behaviour as the B K-edge increase of the 194 eV peak for $LiBH_4$/C deh.+H_2@RT as compared to $LiBH_4$/C deh.: the bands for oxygen from 535 to 530 are more intense (compared to the background noise between 515-530) for $LiBH_4$/C deh.+H_2@RT than for $LiBH_4$/C deh. One should note that these spectra are measured directly after the first B K-edge XRS measurement of the sample (or as second measurement after the treatment). These data do not supply much information on where the oxygenation comes from.

9. C K-edges of $LiBH_4$/C

There are not big changes in the C K-edge XRS of $LiBH_4$/C as prep and after deh and reh as can be seen from the C K-edge XRS spectra in Figure S16.

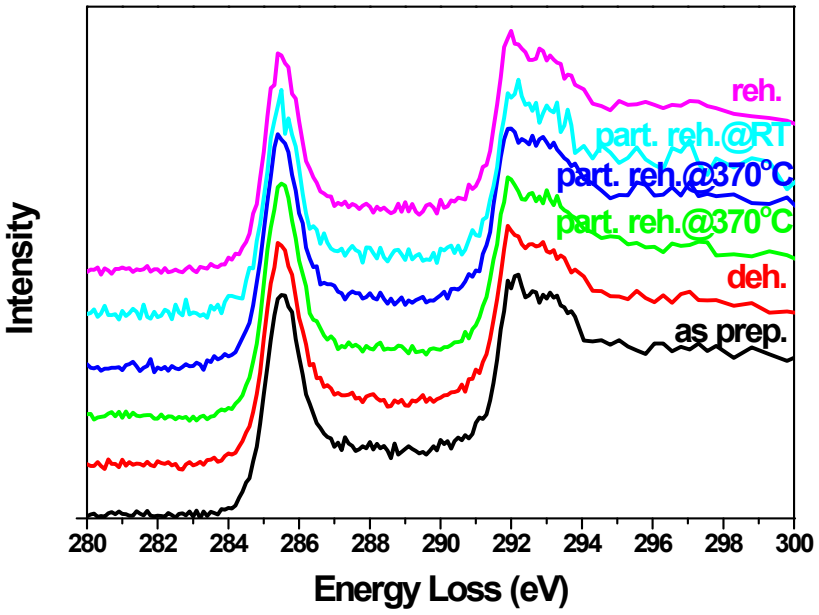

Figure S16. C K-edge XRS of $LiBH_4$/C as prepared (as prep., black), dehydrogenated (deh., red), dehydrogenated and subsequently partially re-hydrogenated by heating to 370°C under 1 bar of hydrogen (part. reh.@370°C, green and blue), and cooled down to room temperature (part. reh.@RT, cyan) and of $LiBH_4$/C re-hydrogenated (reh., magenta).

10. Analysis of $NaBH_4$/C: B and C K-edge XRS and B K-edge XAS calculations

In this section we show that the XRS technique applied to LiBH4/C can also be applied to other systems such as NaBH4/C. Unfortunately we did not have enough beam time to measure good statistics on the $NaBH_4$/C samples as prepared, ex- and in-situ dehydrogenated and ex-situ rehydrogenated. Therefore we only show these in the Supplementary Information, just to show that the XRS technique is transferable to other samples**.**

Preparation of $NaBH_4$/C samples

(1) 25wt% $NaBH_4$/C nanocomposites were prepared by melt infiltration as described previously[1, 2]. In short, 0.25 gram of $NaBH_4$ was mixed with 0.75 g of nanoporous carbon (High surface area graphite: HSAG-500 provided by Timcal Switzerland, pore volume 0.65 cm^3/g, broad pore size contribution, majority of pore sizes is 2-3 nm). The $NaBH_4$-porous carbon mixture was heated to 525 °C in a 4 ml stainless steel Swagelok reactor with an in-situ generated hydrogen of ~ 5 bar (from a reaction between sacrificial $NaBH_4$ and SiO_2 in the first compartment of the reactor). The samples were cooled down under hydrogen pressure and transferred into an argon filled glove box. This sample is further called "$NaBH_4$/C as prep".

(2) Part of the $NaBH_4$/C as prep sample was de-hydrogenated by heating under 25 ml/min argon flow, 5 °C/min with a dwell time of 30 minutes at the maximum de-hydrogenation temperature, 550 °C for $NaBH_4$/C. This de-hydrogenated sample is labelled "$NaBH_4$/C deh".

(3) Part of the $NaBH_4$/C deh was re-hydrogenated by heating in an autoclave to 325 °C under 60 bar hydrogen for 3 hours. These sample will further on be referred to as "$NaBH_4$/C reh".

$NaBH_4$/C XRS measurements

For the nanoconfined sample $NaBH_4$/C, the B and C K-edge XRS of bulk $NaBH_4$ and $NaBH_4$/C as prep, deh and reh ex-situ were measured under helium flow. The $NaBH_4$/C deh sample was also partially re-hydrogenated in-situ by heating under 1 bar of (pure) hydrogen (99.999%) with a flow of 10 ml/min. to 270 °C and after a dwell time of 30 minutes, at this temperature, the B and C K-edge XRS were measured. B and C-K edge XRS were

also acquired for the rehydrogenated sample which was heated to 300 °C and 400 °C, as well as after cooling the sample down to room temperature. The results of the B K-edge XRS of NaBH4/C under these different conditions are shown in Figure S17.

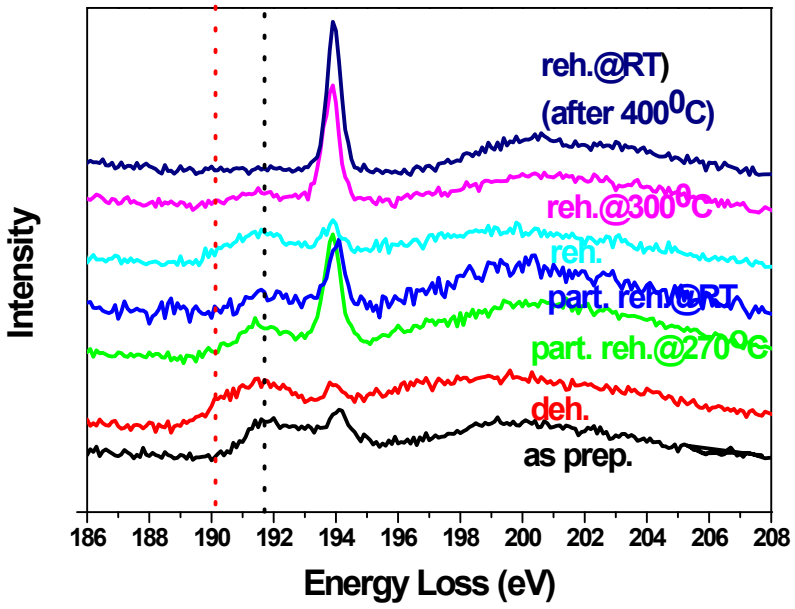

Figure S17. B K-edge XRS of $NaBH_4$/C as prepared (as prep., black), dehydrogenated (deh., red), dehydrogenated and subsequently partially re-hydrogenated by heating to 270°C under 1 bar of hydrogen and kept at 270°C for 30 minutes under hydrogen flow (part. reh.@270°C), green) of the same sample at room temperature after cooling down (part. reh.@RT, blue), $NaBH_4$/C re-hydrogenated (reh., cyan), re-hydrogenated and heated to 300⁰C under helium flow (reh. @300°C, magenta) and re-hydrogenated and dehydrogenated, after heating from 300 to 400⁰C and cooling down to room temperature (reh.(RT) (after 400°C), navy). The vertical black dotted line indicates the peak of the $NaBH_4$/C as prepared. The vertical red dotted line indicates the broad feature that appears in the $NaBH_4$/C dehydrogenated sample.

For a more useful analysis we zoom in on the B K-edge XRS of $NaBH_4$/C as prepared, ex-situ dehydrogenated and ex-situ rehydrogenated in Figure S19 but first we take a look at the B K-edge of the nanoconfined $NaBH_4$/C as prepared in comparison to bulk $NaBH_4$ powder (Figure S18). The spectra of $NaBH_4$/C as prep and $NaBH_4$ bulk look similar, although the $NaBH_4$/C has a stronger band at 194 eV indicating the stronger reaction to oxygen of the nanoconfined sample.

We would like to point out that the B K-edge XRS spectra of bulk $NaBH_4$ (figure Figure S18) and bulk $LiBH_4$ powder (figure 1 in paper, red line) are different, even though they both contain the $[BH_4]^-$ anion. As the XRS technique basically gives electronic information, we can attribute this mainly to the difference in the electronic properties, for example the electro-negativity of the BH_4^- compared to the cations Na^+ and Li^+. Another part that changes the XRS features is the local symmetry and the bonding distances, which are also different for $LiBH_4$ and $NaBH_4$, since the Li+ and Na+ have a different ion radius. To conclude, we can make the distinction in the B K-edge between pure $NaBH_4$ and $LiBH_4$, the XRS technique could also be interesting for studies on mixtures of these two compounds.

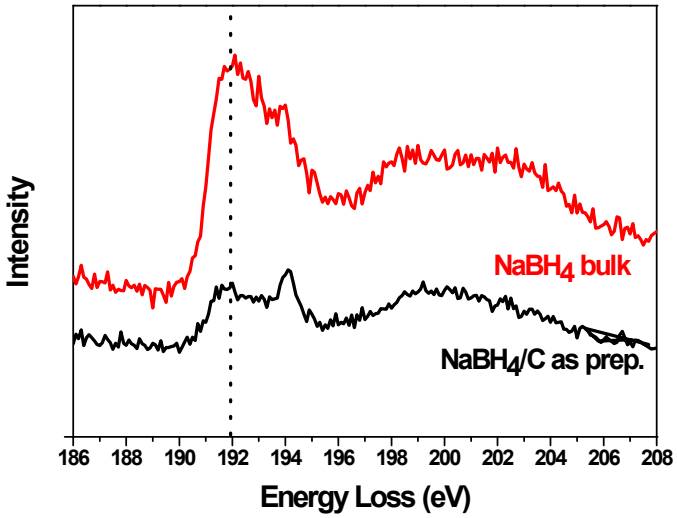

Figure S18. Boron K-edge XRS of $NaBH_4$/C as prepared ($NaBH_4$/C as prep., black) with the bulk $NaBH_4$ powder reference (NaBH4 bulk, red).

B K-edge XRS of $NaBH_4$/C under different conditions

In this subsection we discuss the results of the B K-edge XRS on $NaBH_4$/C. Based on NMR results it has been concluded before that the nanoconfined $NaBH_4$, $NaBH_4$/C, decomposes as follows [11]:

$$12NaBH_4 \rightarrow 10Na + Na_2B_{12}H_{12} + 18H_2 \quad (4a)$$

Although one would expect that for the bulk materials the de-hydrogenation occurs in a similar way as $LiBH_4$:

$$2NaBH_4 \rightarrow 2NaH + 2B + 3H_2 \quad (4b)$$

where NaH can even decompose further: $2NaH \rightarrow 2Na + H_2$ (4c)

In the same paper it was reported that it is possible to re-hydrogenate the $NaBH_4$/C, but only with extra Na added it can almost fully re-hydrogenate (up to 98%)[11]. The obtained hydrogen sorption reversibility for the $NaBH_4$/C is in contrast to bulk $NaBH_4$, where no reversibility of hydrogen sorption has been reported.

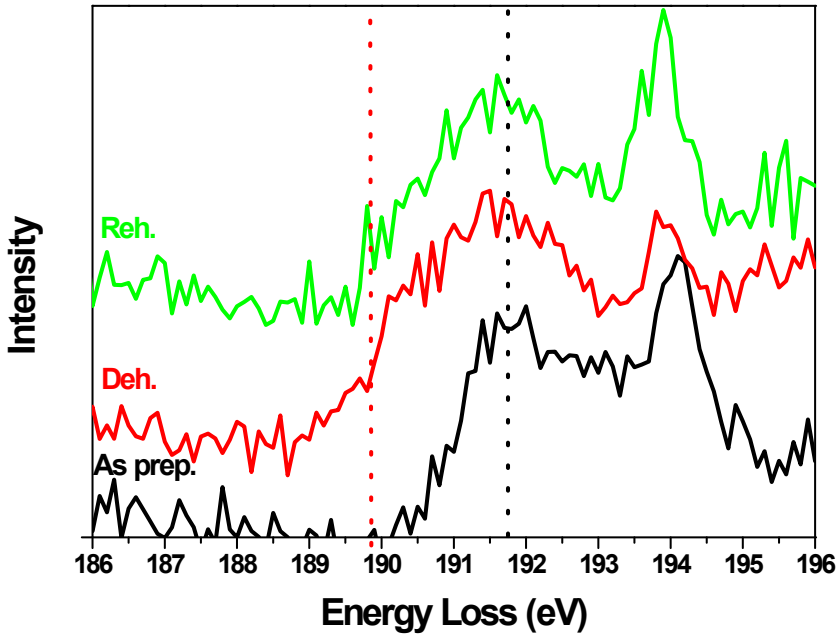

Figure S19. B K-edge XRS of $NaBH_4$/C as prepared (as prep, black) and dehydrogenated $NaBH_4$/C ($NaBH_4$/C deh, red) and ex.situ re-hydrogenated $NaBH_4$/C(reh., green) with energy loss shown to 196 eV. The vertical black dotted line represents the energy loss of the main peak of the spectrum of $NaBH_4$/C as prep and the vertical red dotted line represents the energy of the start of the band of the spectrum of $NaBH_4$/C deh.

Although Figure S19 shows rather noisy data as compared to the shown spectra of $LiBH_4$/C, one can still see that after de-hydrogenation ex-situ by heating to 550 °C under Ar flow, i.e. $NaBH_4$/C deh (red line), the B K-edge XRS spectrum of $NaBH_4$/C deh shows a shift to lower energy compared to the $NaBH_4$/C as prep (black line). Secondly it is noticed that the band becomes broader. Also note that the peak at 194 eV is present for all three spectra, so all the samples were partially oxidized. As mentioned above, it has been recently suggested that Na and $Na_2B_{12}H_{12}$ are the de-hydrogenation products of $NaBH_4$ and $NaBH_4$/C nanocomposites[1, 3, 4].

Since at the time of our measurements, we were not aware of a supplier of commercially available $Na_2B_{12}H_{12}$, we compared the spectra of $NaBH_4$/C deh to XAS calculations which are shown in Figure S20. Note that $Na_2B_{12}H_{12}$ is commercially available nowadays (for example from http://www.katchem.cz/en/products).

In Figure S20 B K-edge XRS spectra of $NaBH_4$/C as prep and deh. are shown in comparison with XAS calculations of $NaBH_4$ and $Na_2B_{12}H_{12}$. The XAS calculations are performed with Quantum-Espresso [5] in the same way as done previously [6] using a boron pseudo-potential with core hole in a $NaBH_4$/$Na_2B_{12}H_{12}$ 2x2x2 supercell calculation. The calculations were performed with the crystal structures of $NaBH_4$ and $Na_2B_{12}H_{12}$ taken from Kumar et al.[7] and Her et al.[8] respectively. The calculated XAS shape of $NaBH_4$ agrees with the experimental XRS of bulk $NaBH_4$ powder, but in the experiment there is also a small contribution of B_2O_3 or $NaBO_2$, since there is a peak visible at 194 eV and the broad band between 196 and 205 eV confirms that there is either some B_2O_3 or $NaBO_2$. Therefore the agreement between calculations and experimental data is not really good. The calculated data have too broad bands, although one has to be careful for the part above 194 eV as the calculations did not include partial oxidation. Nevertheless, the trend between the $NaBH_4$ and $Na_2B_{12}H_{12}$ in the calculations and the trend between the $NaBH_4$/C as prepared and $NaBH_4$/C dehydrogenated is the same: the start of the edge of the calculated XAS of $NaBH_4$ (and the experimental XRS of $NaBH_4$/C as prep) is at higher energies than the XAS of $Na_2B_{12}H_{12}$ (and the experimental $NaBH_4$/C dehydr). Hence, although the calculations do not directly agree with the experiment, but the calculations indicate that in the experimental dehydrogenated $NaBH_4$/C sample $Na_2B_{12}H_{12}$ is found.

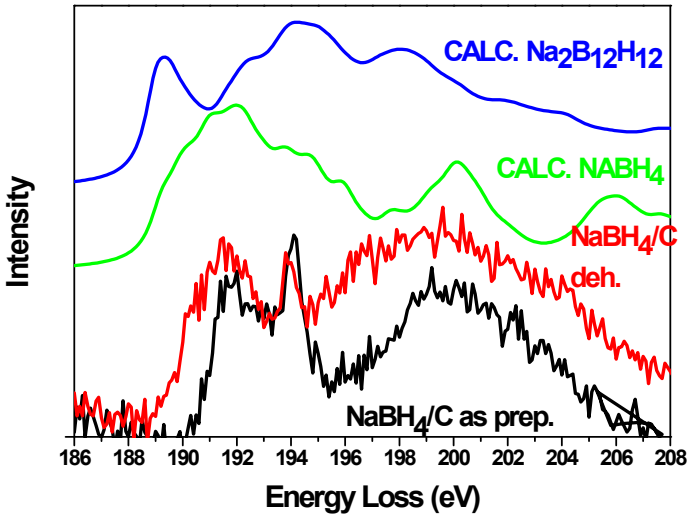

Figure S20. B K-edge XRS of $NaBH_4$/C as prepared ($NaBH_4$/C as prep, black) and dehydrogenated $NaBH_4$/C ($NaBH_4$/C deh, red) and XAS calculations of $NaBH_4$ (green) and $Na_2B_{12}H_{12}$ (blue).

The assignment of mainly $Na_2B_{12}H_{12}$ to the B K-edge XRS of $NaBH_4$/C deh seems valid, although the XAS calculations do not take into account that there is also $NaBO_2$ present. That is one of the reasons why there is no good agreement between calculations and experimental results for $NaBH_4$/C. Nevertheless, the trend between the XAS calculations of $NaBH_4$ and $Na_2B_{12}H_{12}$ and what changes in the spectra of the $NaBH_4$/C as prep compared to the $NaBH_4$/C deh is the same: the start of the edge of the calculated XAS of $NaBH_4$ (and the experimental XRS of $NaBH_4$/C as prep) is at higher energies than the XAS of $Na_2B_{12}H_{12}$ (and the experimental $NaBH_4$/C deh). Hence, although the calculations do not agree well with the experiment, the calculations provide evidence that the features in the experimental XRS of $NaBH_4$/C deh sample can be attributed to $Na_2B_{12}H_{12}$, which is in line with literature. Note that there is possibly also some (possibly something like <10%) boron present in the XRS of $NaBH_4$/C deh.

After rehydrogenation ex-situ, the B K-edge XRS spectrum of $NaBH_4$/C reh shows that the band moves back towards the original on-set of $NaBH_4$/C as prep as shown in figure 5 (reh, green line). However it does not shift back completely. Additionally, the band remains broader, so we conclude that the phase that appears in the de-hydrogenated state is still partially present after re-hydrogenation and this was expected because it was shown before that de-hydrogenated $NaBH_4$ is only partially reversible due to partial loss of Na at high temperature during de-hydrogenation[1]. Thus we conclude that the broad peak after re-hydrogenation is due to reversible formation of $NaBH_4$ from the de-hydrogenation products (Na and $Na_2B_{12}H_{12}$) and the presence of some unconverted $Na_2B_{12}H_{12}$. However, we do confirm that there is partial reversibility to $NaBH_4$, even without adding extra Na.

We also tried in-situ B K-edge XRS measurements during re-hydrogenation of the de-hydrogenated $NaBH_4$/C by heating to 300 °C and 400 °C under 1 bar of hydrogen flow. However unlike $LiBH_4$/C that showed some reversibility at similar conditions, these conditions are not sufficient for the partial re-hydrogenation of $NaBH_4$/C deh. Therefore only increases in the $NaBO_2$ peak were observed (Figure S17, while the $Na_2B_{12}H_{12}$ peak gradually disappeared in the background with time.

In addition, we have attempted to measure Na K-edge XRS on $NaBH_4$/C as prep, but since the signal of XRS depends on the scattering efficiency and because there is more background scattering with higher Z (where Z is the element number) we only measured noise in the Na K-edge XRS around 1000 eV. Note that for the Na K-edge XRS we used all of the rows of the 40-crystal spectrometer, since the Na K-edge signal is expected at larger momentum transfer.

Summarizing, with XRS we find evidence that the $NaBH_4$/C decomposes in $Na_2B_{12}H_{12}$ (and other compounds that do not contain the element boron, for example NaH or Na, but the current measurements cannot say anything about the sodium-containing component). Based on Figure S19 it is concluded that during re-hydrogenation, part of the $Na_2B_{12}H_{12}$ remains, while there is as well $NaBH_4$ appearing again.

C K-edges of $NaBH_4$/C

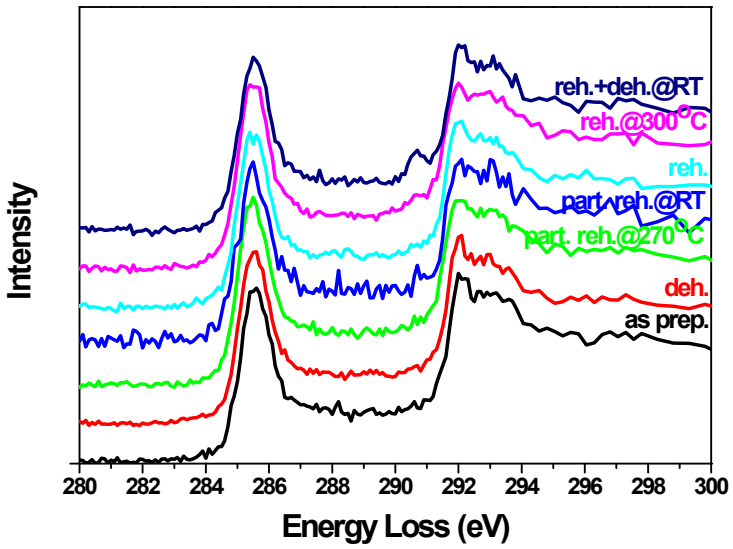

Figure S21. C K-edge XRS of $NaBH_4$/C as prepared (as prep., black), dehydrogenated (deh., red), dehydrogenated and subsequently partially re-hydrogenated by heating under 1 bar of hydrogen to 270°C (part. reh.@270°C, green), and cooled down to room temperature after (part. reh.@RT, blue), re-hydrogenated (reh., cyan), re-hydrogenated, heated to 300°C under helium flow (reh.@300°C, magenta), re-hydrogenated and dehydrogenated again, measurement at room temperature (reh.+deh.@RT, navy).

The C K-edge of $NaBH_4$/C reh and subsequently dehydrogenated again has a clear extra band compared to the $NaBH_4$/C as prep. This could mean there is something going on related to oxygen bonding to the carbon. Since heating was performed in-situ in the cases with these peaks appearing (and only happens for those samples) it can be concluded that oxygenation of the carbon occurs at such elevated temperatures (possibly in combination with an X-ray induced effect).

Overall, it is clear that there are no differences found in the C K-edge XRS of the samples in different stages (as prep, deh and reh) or that at least the differences are tiny and therefore not visible in the measured XRS spectra.

References

1. P. Ngene, R. Van Den Berg, M. H. W. Verkuijlen, K. P. De Jong and P. E. De Jongh, *Energy and Environmental Science*, 2011, **4**, 4108-4115.
2. P. Ngene, R. Van Zwienen and P. E. De Jongh, *Chemical Communications*, 2010, **46**, 8201-8203.
3. R. Caputo, S. Garroni, D. Olid, F. Teixidor, S. Surinach and D. Baro, *Physical Chemistry Chemical Physics*, 2010, **12**, 15093.
4. R. Caputo and A. Züttel, *Molecular Physics*, 2010, **108**, 1263-1276.
5. P. Giannozzi, S. Baroni, N. Bonini, M. Calandra, R. Car, C. Cavazzoni, D. Ceresoli, G. L. Chiarotti, M. Cococcioni, I. Dabo, A. Dal Corso, S. De Gironcoli, S. Fabris, G. Fratesi, R. Gebauer, U. Gerstmann, C. Gougoussis, A. Kokalj, M. Lazzeri, L. Martin-Samos, N. Marzari, F. Mauri, R. Mazzarello, S. Paolini, A. Pasquarello, L. Paulatto, C. Sbraccia, S. Scandolo, G. Sclauzero, A. P. Seitsonen, A. Smogunov, P. Umari and R. M. Wentzcovitch, *Journal of Physics Condensed Matter*, 2009, **21**.

6. P. S. Miedema, P. Ngene, A. M. J. Van Der Eerden, T. C. Weng, D. Nordlund, D. Sokaras, R. Alonso-Mori, A. Juhin, P. E. De Jongh and F. M. F. De Groot, *Physical Chemistry Chemical Physics*, 2012, **14**, 5581-5587.
7. R. S. Kumar and A. L. Cornelius, *Applied Physics Letters*, 2005, **87**.
8. J. H. Her, W. Zhou, V. Stavila, C. M. Brown and T. J. Udovic, *Journal of Physical Chemistry C*, 2009, **113**, 11187-11189.